Determination of the atomic structure of a Gd(1120) surface

1993 J. Phys.: Condens. Matter 5 541

(http://iopscience.iop.org/0953-8984/5/5/005)

J. Phys.: Condens. Matter 5 (1993) 541–550. Printed in the UK

Determination of the atomic structure of a Gd(11$\bar{2}$0) surface

J Quinn†, C P Wang†, F Jona† and P M Marcus‡

† Department of Materials Science and Engineering, State University of New York, Stony Brook, NY 11794, USA

‡ IBM Resarch Center, Yorktown Heights, NY 10598, USA

Received 7 September 1992, in final form 23 November 1992

Abstract. The atomic arrangement on a Gd(11$\bar{2}$0) surface has been determined by means of a quantitative low-energy electron diffraction (LEED) intensity analysis. The surface arrangement is found to be different from bulk structure in two ways: the spacing between the first and the second layer, both of which have two inequivalent atoms in the unit mesh, is contracted by 2.7% (0.05 Å), and the two inequivalent atoms in the first layer translate parallel to the surface by equal and opposite amounts of 0.10 Å. Thus the change in registration of the composite surface layer preserves both the size and the symmetry of the unit mesh of parallel bulk layers. This kind of surface rearrangement is a relaxation, and is very similar to the relaxation found on Tb(11$\bar{2}$0), but quite different from the reconstruction found by others on (11$\bar{2}$0) surfaces of some other rare-earth metals such as Y, Ho and Er.

1. Introduction

The (11$\bar{2}$0) surfaces of hexagonal close-packed (HCP) crystals are interesting because, in contrast to the (0001) surfaces, their unit mesh has two non-equivalent atoms which can relax differently. There are two previous structural analyses of HCP(11$\bar{2}$0) surfaces, namely Co(11$\bar{2}$0) [1] and Tb(11$\bar{2}$0) [2]. On Co(11$\bar{2}$0) the internal coordinate between the two non-equivalent atoms does not change, but on Tb(11$\bar{2}$0) the coordinate changes by equal and opposite displacements of the two basis atoms parallel to the surface plane.

Other HCP(11$\bar{2}$0) surfaces seem to be anomalous. Qualitative LEED studies of the (11$\bar{2}$0) surfaces of Y, Ho and Er have indicated that these surfaces are reconstructed to resemble the (0001) surfaces [3,4], although Y(11$\bar{2}$0) also exhibits the relaxed surface structure [5].

The question of whether the reconstructions of the (11$\bar{2}$0) surfaces of Y, Ho and Er are the exception or the rule in the family of rare-earth metals is unanswered at this point. The experiments are complicated by the fact that single crystals of the rare earths are difficult and expensive to get with high purity [6,7], while the surfaces of even ultrahigh-purity crystals of these elements are very difficult to prepare in the atomically clean state [8], primarily because of the segregation of iron from the bulk [2,9].

In the work on a (11$\bar{2}$0) surface of Gd reported here we have succeeded in cleaning the surface to an acceptable level and we have carried out a LEED experiment and an intensity analysis in order to determine the structure of this surface. In

0953-8984/93/050541+10$07.50

section 2 we describe the bulk structure of Gd(11$\bar{2}$0) and the notation used in this paper. In section 3 we detail the procedure followed for the preparation of an atomically clean surface. In section 4 we report on the intensity calculations, the structure analysis and its results, and in section 5 we summarize and discuss the results.

2. Bulk structure of Gd(11$\bar{2}$0)

The lattice parameters of HCP Gd are $a = 3.64$ Å and $c = 5.78$ Å, hence the axial ratio $c/a = 1.588$. A cut through a hard-sphere model of bulk Gd along a (11$\bar{2}$0) plane is depicted in figure 1 ((*a*) top view, (*b*) side view).

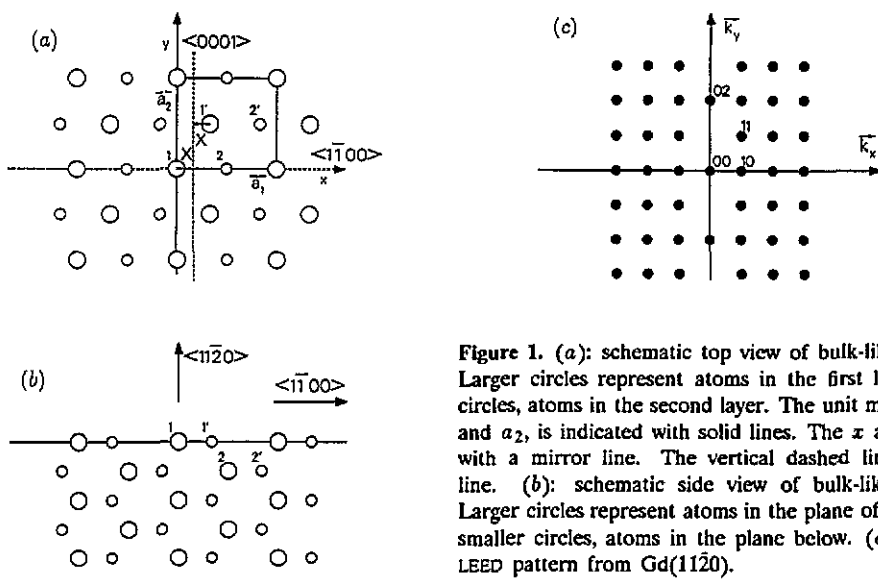

Figure 1. (*a*): schematic top view of bulk-like Gd(11$\bar{2}$0). Larger circles represent atoms in the first layer, smaller circles, atoms in the second layer. The unit mesh, sides a_1 and a_2, is indicated with solid lines. The x axis coincides with a mirror line. The vertical dashed line is a glide line. (*b*): schematic side view of bulk-like Gd(11$\bar{2}$0). Larger circles represent atoms in the plane of the drawing, smaller circles, atoms in the plane below. (*c*): schematic LEED pattern from Gd(11$\bar{2}$0).

We choose a Cartesian coordinate system with x and y in the (11$\bar{2}$0) plane, the x axis along ⟨1$\bar{1}$00⟩, the y axis along ⟨0001⟩, and a z axis along [11$\bar{2}$0], as indicated in the figure. The surface unit mesh is a rectangle with sides $a_1 = 2a \sin 60° = 6.3047$ Å and $a_2 = c = 5.78$ Å, and contains two atoms (labelled 1 and 1′ in figure 1(*a*)) with coordinates (0,0) and $(a_1/3, a_2/2)$, respectively. The symmetry elements are: a mirror plane (line) perpendicular to ⟨0001⟩ (dashed line coinciding with the x axis in figure 1(*a*)) and a glide plane (line) parallel to ⟨0001⟩ at location $x = a_1/6$ (vertical dashed line in figure 1(*a*)). The translation vector from the origin in the first to the origin in the second layer is $s = (a_1/2, 0, -d_{\text{bulk}})$ with $d_{\text{bulk}} = a/2 = 1.82$ Å.

The geometry of the LEED pattern from Gd(11$\bar{2}$0) is shown schematically in figure 1(*c*). The mirror line along k_x makes corresponding reflections above and below that line degenerate to one another. In addition, systematic reflection absences are expected as a consequence of the glide line: with the choice of axes made in figure 1, absences are expected (and observed) in the beams with indices $0k$ with k

odd. Additional extinctions would be expected to occur in the kinematic limit for an ideally bulk-like surface, owing to the special relative positions of atoms 1 and 1′, at the reflections hk such that $h/3 + k/2 = n + 1/2$, i.e. with $h = 3n$, n a non-zero integer, and k odd. These extinctions are not observed, however, for two reasons. The first reason is multiple scattering: even for an ideally bulk-like surface a dynamical calculation shows that the reflection 31, for example, is weak, but not zero. The second reason is that on the $(11\bar{2}0)$ *surface* the relative positions of atoms 1 and 1′ can vary, expectedly in such a way that both the mirror line and the glide line are maintained. For example, calling the shortest distance from atom 1 and from atom 1′ to the glide line X (see figure 1(*a*), $X = a_1/6 = 1.05$ Å in the ideally bulk-like structure), a change ΔX of X would violate the extinction condition and produce a non-zero intensity in, e.g., the 31 reflection. We will see below that, in fact, ΔX is finite on the Gd$(11\bar{2}0)$ surface.

3. Experimental details

A single-crystal ingot of Gd metal, purified by the method of solid-state electrotransport as described elsewhere [7], was oriented along a $\langle 11\bar{2}0\rangle$ direction by means of Laue diffraction patterns. A platelet with semicircular shape, approximately 4 mm in diameter and 1 mm in thickness, and with the major surfaces perpendicular to a $\langle 11\bar{2}0\rangle$ direction, was then cut with a slow diamond wheel. One of the two $(11\bar{2}0)$ surfaces was lapped and polished in kerosene with diamond-powder slurries with successively decreasing grain sizes (3, 1 and 0.25 μm) until the orientation was within 0.5° of a $(11\bar{2}0)$ plane. The platelet was then mounted in a sample holder which allowed heating of the platelet by electron bombardment of the back surface.

After attainment of base pressure ($< 5 \times 10^{-10}$ Torr), the polished surface was subjected to repeated bombardments with Ar ions (5×10^{-5} Torr, 375 V, 2 μA) as described below, and was tested for impurities by Auger electron spectroscopy (AES) using the LEED optics as a retarding-field analyser (RFA) and a grazing-incidence electron gun operated at 3000 V. Figure 2 depicts, on top, an AES scan taken immediately after bakeout of the experimental chamber and before any cleaning procedure, representing therefore the starting condition of the surface (large Cl and O signals are visible). The concentrations of the main impurities, Fe, Cl, C, and O, were monitored by the ratio R_X between the intensity of the AES line of impurity X (Fe at 47 eV, Cl at 181 eV, C at 272 eV, and O at 512 eV) to the intensity of the AES line of Gd at 138 eV.

Six hours of Ar-ion bombardment of the surface at room temperature produced a relatively clean surface with $R_{Cl} = I_{Cl(181)}/I_{Gd(138)} = 0.0$, $R_C = I_{C(272)}/I_{Gd(138)} = 0.07$, $R_O = I_{O(512)}/I_{Gd(138)} = 0.0$ and $R_{Fe} = I_{Fe(47)}/I_{Gd(138)} = 0.0$. However, after a 1 h anneal at 600 °C the Cl and C impurities increased again to $R_{Cl} = 1.25$ and $R_C = 0.23$. Seven cycles of 1/2 h Ar bombardments followed by anneals at increasing temperatures between 600 and 1000 °C, ranging in time between minutes and hours, were needed to reduce the Cl, C and O impurities to acceptable levels ($R_{Cl} = 0.02$, $R_C = 0.04$, $R_O = 0.0$, and $R_{Fe} = 0.03$). No acceptable LEED pattern was observed until these low levels were reached, and good quality LEED patterns required prolonged annealings. However, after the reduction of the Cl concentration the annealing treatments caused a notable increase of the Fe concentration—a phenomenon that we had observed earlier in experiments on both Gd and Tb surfaces

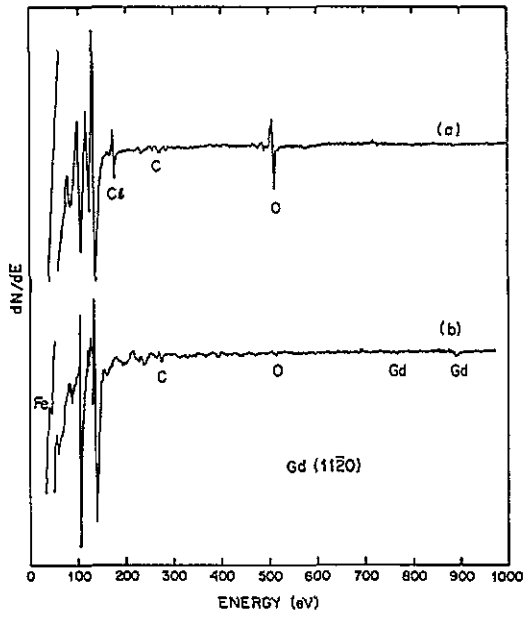

Figure 2. AES scans of Gd(11$\bar{2}$0): (*a*) initial condition; (*b*) 'clean' condition after the procedure described in the text. The unmarked AES lines are Gd lines.

[2, 9, 10]. For example, after depletion of Cl, a 10 min anneal at 600 °C increased R_{Fe} to 0.25. The segregation of Fe on the surface was of course a function of temperature and time: at 400 °C, R_{Fe} would rise to 0.05 after 10 min, to 0.18 after an additional 30 min, and to 0.30 after an additional $1\frac{1}{2}$ h. This behaviour is different from that observed on Tb(11$\bar{2}$0), where 3 h anneals at 400 °C produced good LEED patterns with no visible Fe signal in AES scans [2].

The procedure that was finally adopted in this work, *after* all the treatments described above, in order to prepare a 'clean' and well-ordered Gd(11$\bar{0}$2) surface is the following: Ar-ion bombardment of the surface at room temperature for 20 min, anneal to 1000 °C for 1 min followed by rapid cooling to room temperature (the surface temperature dropped to 700 °C in the first 10 s). After this procedure the impurities' AES ratios on the surface were typically (as obtained, e.g., from figure 2) $R_{Fe} = 0.03$, $R_{Cl} = 0.0$, $R_C = 0.04$ and $R_O = 0.02$, a condition that we define as 'clean' in the present work [11]. A typical AES spectrum of such a 'clean' surface is depicted in figure 2, bottom. We note the presence of a peak at 60 eV which was not visible immediately after bakeout (figure 2, top), but was always present, after cleaning, independently of the bombardment or annealing treatments applied. Such a peak was not observed on Gd(0001) [10], so its origin is not wholly clear at this time. It may in fact not be associated with Auger effects at all: it may be due to the diffraction of secondary electrons, as has been observed in experiments on Cu and Co [12], and on Mg and MgO [13].

The LEED patterns observed after the procedure described above were good up to electron energies of about 150 eV, whereafter the background increased noticeably. Attempts to improve the surface order, either by prolonging the anneals at 1000 °C or

by annealing at lower temperatures for different times, failed and resulted in increased segregation of Fe and C on the surface. (We note again that on Tb(11$\bar{2}$0) the LEED patterns were acceptable up to about 300 eV, although intensity data could be reliably collected only up to about 200 eV.) The LEED $I(V)$ spectra were always reproducible after the cleaning procedure described in the preceding paragraph. For the purposes of intensity analysis the following nine $I(V)$ spectra were obtained by averaging corresponding degenerate spectra collected (with a microcomputer–television-camera system described elsewhere [14]) from 24 to 180 eV at normal incidence of the primary electron beam: 10, 11, 20, 02, 21, 12, 22, 30 and 13. (The 31 beam, which should be particularly sensitive to the distance X of atoms 1 and 1′ from the glide line, see section 2, was not used in the analysis because its intensity was very low and therefore not measurable with sufficient accuracy.) These spectra were then normalized to constant incident current, smoothed (by convolution of the experimental curves with Gaussian filter functions) and corrected to reduce the background to a minimum. The symmetry relations among the beams told us that the two symmetry elements of the bulk planes (mirror and glide) were present in the surface as well.

4. Structure analysis and results

The calculations of LEED intensities were performed with the CHANGE computer program [15]. This program treats the scattering from each composite layer, made up of two elementary or Bravais nets in the same plane, in spherical waves, and the scattering between composite layers in plane waves (beams).

A Gd potential was calculated from relativistic charge densities kindly provided by N E Christensen. The intensity calculations were done either with relativistic phase shifts calculated from this potential with a program provided by D D Koelling [16] or with non-relativistic phase shifts calculated from the same potential. No differences were detected between $I(V)$ curves calculated either way. We used either eight or ten phase shifts, which produced negligible differences in the intensities of some peaks, and 141 beams for calculations up to 180 eV.

The inner potential was chosen initially to be $V_0 = -(10 + 4\mathrm{i})$ eV, but the real part was varied as a fitting parameter in the course of the analysis. The final value was $V_0 = -(7 + 4\mathrm{i})$ eV with an error of ± 3 eV in the real part. The amplitude of the atomic vibrations was taken as $\langle u^2 \rangle^{1/2} = 0.10$ Å, corresponding to a Debye temperature of 152 K.

The structure analysis concentrated initially on varying the first interlayer spacing d_{12} and the registration X of the top layer (see section 2). The changes in these parameters from the bulk values $d_{12} = 1.82$ Å and $X = a_1/6 = 1.05$ Å are labelled Δd_{12} and ΔX, respectively, a positive value of ΔX indicating shifts of atoms 1 and 1′ along x away from the glide line. The initial variations spanned the following ranges: for Δd_{12} from -0.20 to $+0.20$ Å in steps of 0.05 Å, and ΔX from -0.20 to $+0.30$ Å in steps of 0.10 Å.

The evaluation of the fit between theory and experiment was done both visually and by means of three reliability factors, namely, R_{VHT} [17], r_{ZJ} [18] and R_{P} [19].

Initially, calculations done with eight non-relativistic phase shifts were plagued by numerical instabilities at several energy values. This condition was only marginally improved by the use of either ten non-relativistic or eight or ten relativistic phase shifts. The results became acceptably stable when two layers (four atoms), i.e. the top

and the second layer, were included in the spherical-wave representation, as opposed to the top layer (two atoms) only.

The fit to experiment was never wholly satisfactory; nevertheless, all R factors were minimized for a small contraction of the first interlayer spacing and a positive value of ΔX. The refinement included variations of the second interlayer spacing d_{23}, with Δd_{23} varying from -0.08 to $+0.08$ Å in steps of 0.02 Å. Contour plots of all three R factors in the Δd_{12}–Δd_{23} plane and in the ΔX–Δd_{23} plane are depicted in figures 3 and 4, respectively. We note that the R_P and r_{ZJ} minima are high, and the structural parameters that produce the three minima scatter from one another by as much as 0.05 Å for the interlayer spacings and by as much as 0.14 Å for the ΔX parameter.

In the absence of an explanation for the mediocre quality of the agreement between theory and experiment (see section 5), we chose to average the parameter values that produced the individual R factor minima to a final set as follows:

$$\Delta d_{12} = -0.05 \pm 0.03 \text{ Å (2.7\% compression)}$$
$$\Delta d_{23} = -0.02 \pm 0.03 \text{ Å (1\% compression)}$$
$$\Delta X = +0.10 \pm 0.10 \text{ Å(about 10\% increase in } X).$$

The error bars have been estimated to include all parameter values which minimize the three R factors, and for Δd_{12} and Δd_{23} they have the magnitudes of the error bars found in earlier error analyses in LEED crystallography [20]. For the lateral translation ΔX the error bar is larger, predominantly because normal-incidence LEED is not very sensitive to in-plane atom displacements. Nevertheless, the $I(V)$ curves calculated for $\Delta X = 0$ (not shown here) visibly produce a much worse fit to experiment than those calculated for $\Delta X = 0.10$ Å—a fact that can be confirmed by a study of the contour plots for r_{ZJ} and R_{VHT} depicted in figure 4. The failure of R_P to yield results similar to those produced by the other two R factors, in this case, is not understood. It is however not uncommon, in our experience, for one the three R factors to produce results in contrast to the other two—in general, each R factor weighs somewhat different characteristics of the $I(V)$ spectra and there is no *a priori* reason for preferring one R factor over the others.

Figure 5 juxtaposes the experimental and the theoretical $I(V)$ spectra calculated for the parameter values listed above. The overall R factor values for the curves shown in figure 5 are: $R_P = 0.42$, $r_{ZJ} = 0.29$, and $R_{VHT} = 0.25$.

5. Discussion and conclusions

The agreement between theory and experiment is not very satisfactory—it is in fact visibly worse than that obtained in the analysis of Tb(11$\bar{2}$0); see, in particular, the 02 and the 22 spectra. We have not been able to establish the reasons for this fact and have not succeeded in improving the agreement [21]. We repeatedly re-examined the experimental data, especially in the energy ranges where the largest discrepancies between theory and experiment were detected, but always reconfirmed the experimental spectra as shown in figure 5. We also varied to a reasonable extent several non-structural parameters, in particular, as mentioned above, the number (eight or ten) and the nature (relativistic or non-relativistic) of the Gd phase shifts, and the number of atoms (two or four) included in the surface region that is treated

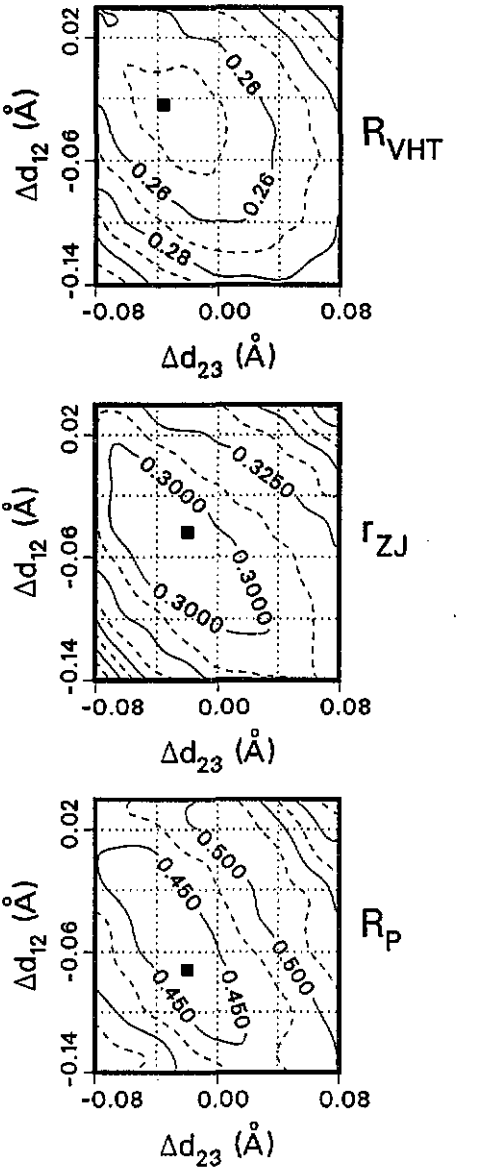

Figure 3. Contour plots of the van Hove–Tong R_{VHT}, the Zanazzi–Jona r_{ZJ} and the Pendry R_P reliability factors in the Δd_{12}–Δd_{23} plane. The minimum values are indicated by the small squares.

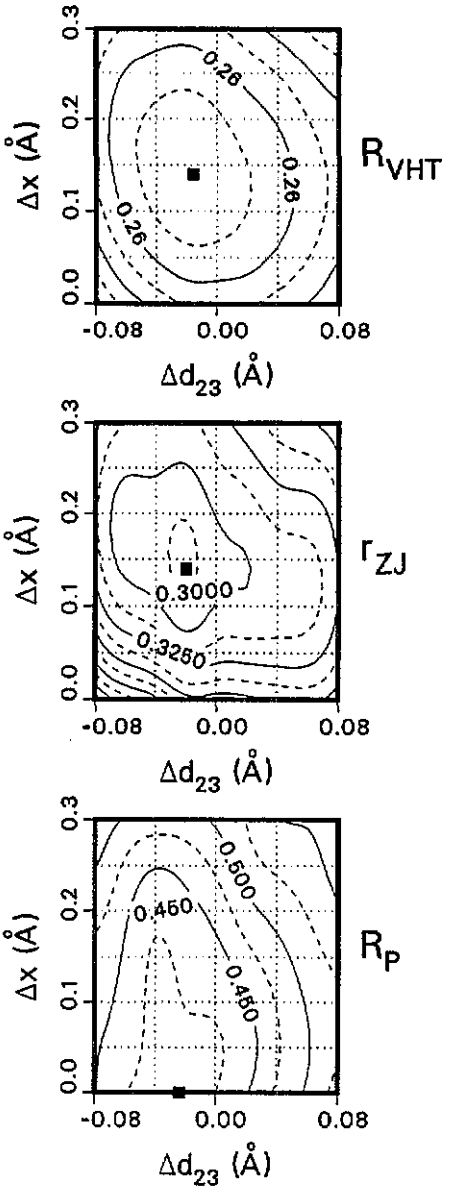

Figure 4. Contour plots of the van Hove–Tong R_{VHT}, the Zanazzi–Jona r_{ZJ} and the Pendry R_P reliability factors in the ΔX–Δd_{23} plane. The minimum values are indicated by the small squares.

in the spherical-wave expansion in the calculations. The relatively high values of the final R factors confirm the visual judgment of mediocre agreement between theory and experiment.

The results quoted above appear nevertheless significant, and it is appropriate to make them available at this time in view of the paucity of results available for other

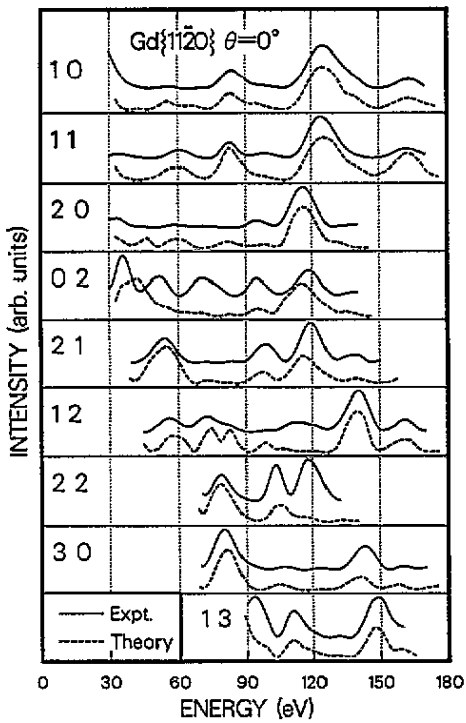

Figure 5. Experimental and theoretical LEED $I(V)$ spectra for normal incidence on Gd(11$\bar{2}$0).

HCP(11$\bar{2}$0) surfaces. The present results for Gd(11$\bar{2}$0) may be compared to those for Tb(11$\bar{2}$0). These two surfaces have similar relaxations: a small contraction of the first interlayer spacing (2.7% for Gd(11$\bar{2}$0) and 3.3% for Tb(11$\bar{2}$0)); a smaller contraction of the second interlayer spacing (1% for Gd(11$\bar{2}$0) and 0% for Tb(11$\bar{2}$0), but it should be stated that the second interlayer spacing was not varied in the Tb analysis since the fit to experiment was already quite satisfactory), and a change in registration of the two sublayers in the top (composite) layer (0.1 Å for Gd(11$\bar{2}$0) and 0.21 for Tb(11$\bar{2}$0)). The change in registration is such that the symmetry elements present on bulk (11$\bar{2}$0) planes (a mirror and a glide line) are maintained.

Thus, on Gd(11$\bar{2}$0), like on Tb(11$\bar{2}$0), the surface relaxation is more complex than on cubic metal surfaces in that it involves a composite layer made up of two elementary or Bravais nets which translate differently, and thereby change an internal structural parameter—the position vector of the second atom in the basis. This more general relaxation does not seem to occur on Co(11$\bar{2}$0) [1], which exhibits a contraction of 8.5% of the first interlayer spacing, but no parallel translation of either atom in the basis, i.e. no change of registration.

Finally, we note that the present results differ from those reported by the Liverpool group [3,4] for Y(11$\bar{2}$0), Ho(11$\bar{2}$0) and Er(11$\bar{2}$0), which are reconstructed. The reasons for this difference are unknown at this time.

Acknowledgments

We acknowledge partial support of this work by the Department of Energy with Grant DE-FG02-86ER45239 and by the National Science Foundation with Grant DMR-8921123. The sample used in this work resulted from joint rare-earth-purification research at Birmingham and Iowa State Universities, funded by the UK Science and Engineering Research Council and by the US Department of Energy, respectively. We are indebted to D Fort for providing the sample and to N E Christensen for providing the relativistic charge densities of Gd.

References

[1] Welz M, Moritz W and Wolf D 1983 *Surf. Sci.* **125** 473
[2] Li Y S, Quinn J, Jona F and Marcus P M 1992 *Phys. Rev.* B **46** 30
[3] Blyth R I R, Cosso R, Dhesi S S, Newstead K, Begley A M, Jordan R G and Barrett S D 1991 *Surf. Sci.* **251/252** 722
[4] Barrett S D, Blyth R I R, Begley A M, Dhesi S S and Jordan R G 1991 *Phys. Rev.* B **43** 4573 and references therein
[5] Barrett S D, Jordan R G and Begley A 1987 *J. Phys. F: Met. Phys.* **17** L145
[6] Beaudry B J and Gschneidner K A Jr 1987 *Handbook on the Physics and Chemistry of Rare Earths* vol 1 ed K A Gschneidner Jr and L Eyring (Amsterdam: North Holland) p 173
[7] Fort D 1987 *J. Less-Common Met.* **134** 45
[8] Netzer F P and J Matthew A D 1986 *Rep. Progr. Phys.* **49** 621
[9] Wu S C, Li H, Tian D, Quinn J, Li Y S, Jona F, Sokolov J and Christensen N E 1990 *Phys. Rev.* B **41** 11911
Wu S C, Li H, Li Y S, Tian D, Quinn J, Jona F, Fort D and Christensen N E 1992 *Phys. Rev.* B **45** 8867
[10] Quinn J, Li Y S, Jona F and Fort D 1992 *Phys. Rev.* B **46** 9694
[11] An attempt at quantifying the actual concentrations of impurities on these 'clean' surfaces could be made by using a formula for quantitative analysis as given in the Auger Handbook (Davis L E, MacDonald N C, Palmberg P W, Riach G E and Weber R E 1978 *Handbook of Auger Electron Spectroscopy* (Eden Prairie, Mn: Physical Electronics Industries, Inc.)). This formula requires knowledge of the 'relative sensitivities' between the elements involved (in the present case, C, O, Fe, Gd) and Ag—sensitivities which can be obtained from the AES Handbook itself. Using this formula we find the following typical concentrations, in atomic per cent: C 4%, O 1%, Fe 2% and Gd 93%. However, these estimates are uncertain for at least two reasons.
(1) The 'sensitivities' obtained from the AES Handbook were determined with a cylindrical-mirror analyser (CMA), whereas our data were obtained with the LEED optics used as a retarding-field analyser (RFA). The RFA is much more sensitive than the CMA for low-energy AES lines such as the Fe line at 47 eV, hence the above 2% estimate for Fe is too large.
(2) The sensitivity for Gd as obtained from the AES Handbook is clearly not correct, since the AES spectrum for Gd in the Handbook shows that the Gd surface examined in *that* experiment was very 'dirty' (large C and O AES lines). We can therefore only *estimate* that the impurity concentrations on the 'clean' surfaces of Gd($11\bar{2}0$) studied in this work were approximately 1% or less for O and Fe, and between 2 and 5% for C.
[12] McDonnell L, Powell B D and Woodruff D P 1973 *Surf. Sci.* **40** 669
[13] Janssen A P, Schoonmaker R C, Chambers A and Prutton M 1974 *Surf. Sci.* **45** 45
[14] Jona F, Strozier J A Jr and Marcus P M 1985 *The Structure of Surfaces* ed M A Van Hove and S Y Tong (Berlin: Springer) p 92
[15] Jepsen D W 1980 *Phys. Rev.* B **22** 5701, 814
[16] Koelling D D and Harmon B N 1977 *J. Phys. C: Solid State Phys.* **10** 3107
[17] Van Hove M A, Tong S Y and Elconin M H 1977 *Surf. Sci.* **64** 85
[18] Zanazzi E and Jona F 1977 *Surf. Sci.* **62** 61
[19] Pendry J B 1980 *J. Phys. C: Solid State Phys.* **13** 937
[20] Jona F, Jiang P and Marcus P M 1987 *Surf. Sci.* **192** 414

[21] One difference between Gd and Tb that may possibly affect the LEED data could be that the Gd surface was ferromagnetic with a surface Curie temperature higher than the bulk Curie temperature of 293 K (Weller D and Alvarado S F 1988 *Phys. Rev.* B 37 9911), whereas the Curie temperature of Tb is well below room temperature ($\simeq$ 220 K). We note, however, that in the study of Tb(11$\bar{2}$0) [2] no differences were found in the $I(V)$ spectra taken at room temperature or at 150 K.